Original Article

Connecting the dots: (RANKL$^+$) extracellular vesicle count in blood plasma in relation to bone metastases, skeletal related events and osimertinib treatment in patients with EGFR mutated non-small cell lung cancer

Anita J. W. M. Brouns[1,2,3], Iris J. Robbesom-van den Berge[4], Sophie M. Ernst[5], Christi M. J. Steendam[5], Wouter W. Woud[6], Liang Wu[7], Anne-Marie C. Dingemans[5], Lizza E. L. Hendriks[2,3], Marjolein van Driel[4]

[1]Department of Respiratory Medicine, Zuyderland, Geleen, The Netherlands; [2]Department of Respiratory Medicine, Maastricht University Medical Center+, Maastricht, The Netherlands; [3]GROW-School for Oncology and Reproduction, Maastricht, The Netherlands; [4]Department of Internal Medicine, Erasmus Medical Center, Rotterdam, The Netherlands; [5]Department of Respiratory Medicine, Erasmus Medical Center Cancer Institute, University Medical Center, Rotterdam, The Netherlands; [6]Department of Neurosurgery, Brain Tumor Center, Erasmus Medical Center, The Netherlands; [7]Erasmus MC Transplant Institute, Department of Internal Medicine, University Medical Center, Rotterdam, The Netherlands

Contributions: (I) Conception and design: AJWM Brouns, AMC Dingemans, LEL Hendriks, M van Driel; (II) Administrative support: AJWM Brouns; (III) Provision of study materials or patients: SM Ernst, CMJ Steendam, WW Woud, L Wu; (IV) Collection and assembly of data: AJWM Brouns, IJ Robbesom-van den Berge, SM Ernst; (V) Data analysis and interpretation: AJWM Brouns, IJ Robbesom-van den Berge, LEL Hendriks, M van Driel; (VI) Manuscript writing: All authors; (VII) Final approval of manuscript: All authors.

Correspondence to: Marjolein van Driel, PhD. Department of Internal Medicine, Erasmus Medical Center, Dr. Molewaterplein 40, 3015 GD Rotterdam, The Netherlands. Email: m.vandriel@erasmusmc.nl.

Background: The biological mechanisms responsible for the different incidences of bone metastases in molecular subgroups of non-small cell lung cancer (NSCLC) are not identified. Extracellular vesicles (EVs) may play a role, as they are involved in organotrophic metastasis. Phosphorylation of epidermal growth factor receptor (EGFR) in exosomes possibly leads to an increase in receptor activator of nuclear factor κB ligand (RANKL) triggering osteoclastogenesis. In search for new biomarkers with focus on EVs and RANKL, we studied in plasma of patients with *EGFR*$^+$ NSCLC the associations between the total concentration of EVs, RANKL$^+$ EVs, RANKL, and osteoprotegerin (OPG) protein levels, osimertinib treatment, presence of bone metastases and skeletal related events (SREs).

Methods: From the prospective biomarker cohort study START-TKI (NCT05221372), including patients with metastatic *EGFR*$^+$ NSCLC, we collected deep frozen plasma samples at initiation and during osimertinib treatment. Imaging flow cytometry (IFC) was used to determine the concentration of tetraspanin positive EVs and detection of RANKL on EVs. RANKL and OPG levels were measured by enzyme-linked immunosorbent assay (ELISA). Data on demographics, date of NSCLC diagnosis, date of initiation of osimertinib, presence of bone metastases and SREs were collected. Primary endpoint was the relation between (RANKL$^+$) EV levels and bone metastases.

Results: Forty unique patients with in total 50 plasma samples (45% at initiation of osimertinib, 55% during osimertinib treatment) were included. Identification of EVs was possible in 38/40 patients, and determination of RANKL and OPG plasma levels in all samples. Of these 40 patients, 25 (63%) had bone metastases at sample collection. Both total EV and RANKL$^+$ EV concentrations were significantly higher in samples at initiation of osimertinib compared to samples during treatment [mean ± standard deviation (SD), $6.3\times10^{12}\pm2.1\times10^{12}$/mL plasma *vs.* $3.2\times10^{12}\pm1.9\times10^{12}$/mL plasma, $P\leq0.001$ for total EV concentrations; and $2.2\times10^{10}\pm9.3\times10^{9}$/mL plasma *vs.* $1.1\times10^{10}\pm8.0\times10^{9}$/mL plasma, $P=0.001$ for RANKL$^+$ EVs]. Patients without a SRE had a significantly higher concentration of RANKL$^+$ EVs compared to patients with an SRE (mean ± SD, $1.8\times10^{10}\pm1.1\times10^{10}$/mL plasma *vs.* $1.1\times10^{10}\pm7.4\times10^{9}$/mL plasma, $P=0.02$). No association was found between the total EV concentration or RANKL$^+$ EVs, plasma levels of OPG and RANKL and bone metastases.

Conclusions: No association was found between the presence of bone metastases and the total concentration of EVs, RANKL+ EVs, or plasma values of RANKL and OPG. In patients without SREs the concentration of RANKL+ EVs was significantly increased. Both the total EV and RANKL+ EV concentrations significantly decreased during osimertinib treatment. This opens new perspectives for the role of (RANKL+) EVs as prognostic biomarkers for *EGFR*+ NSCLC disease progression and response to therapy.

Keywords: Bone metastases; extracellular vesicles (EVs); epidermal growth factor receptor+ non-small cell lung cancer (*EGFR*+ NSCLC); receptor activator of nuclear factor κB ligand (RANKL); osteoprotegerin (OPG)

Submitted Oct 25, 2024. Accepted for publication Jan 24, 2025. Published online Mar 19, 2025.
doi: 10.21037/tlcr-24-1007
View this article at: https://dx.doi.org/10.21037/tlcr-24-1007

Introduction

Background

Approximately half of the patients with non-small cell lung cancer (NSCLC) have metastases at diagnosis (1,2). The biological mechanisms underlying the predilection of tumor cells to metastasize to a specific organ are complex (3,4). Understanding these mechanisms could provide valuable insights for identifying and potentially prophylactically treating patients at increased risk for certain organ metastasis. Previously, we found an association between epidermal growth factor receptor (*EGFR*)+ mutated NSCLC and an increased incidence of bone metastases compared with other molecular subtypes (5). We aimed to identify the underlying biological mechanisms responsible for these differences by performing tumor tissue analysis of EGFR, receptor activator of nuclear factor κB (RANK), RANK ligand (RANKL), and osteoprotegerin (OPG) gene expression. This showed that patients with bone metastases had an increased RANKL gene expression and RANKL:OPG ratio, but we could not demonstrate differences between patients of other molecular subtypes (6). As EGFR signaling is involved in RANKL-mediated osteoclast differentiation and survival, we hypothesized that there could be a relation between upregulated EGFR expression (which could result in increased EGFR signaling) and bone metastases (7-9). Although *EGFR* gene expression was increased in the *EGFR*+ subgroup, bone metastases and *EGFR* gene expression were not associated with each other (6). A key limitation of this study was the small sample size, mainly due to the lack of sufficient tumor tissue in the available biopsies, which resulted in limited statistical power. The lack of sufficient tumor tissue after performing all standard diagnostic procedures for biomarker analysis is a frequently encountered problem in translational research, and less invasive methods are needed (10). The use of liquid biopsies is increasing in molecular analysis and disease monitoring. Therefore, it would be of great clinical use if the biological behavior of a tumor could be predicted via

Highlight box

Key findings

- Total extracellular vesicle (EV) count and receptor activator of nuclear factor κB ligand (RANKL)+ EV count in plasma significantly decreased during osimertinib treatment in epidermal growth factor receptor (*EGFR*)+ mutated non-small cell lung cancer (NSCLC). No association was found between bone metastases and (RANKL+) EV count, plasma values of RANKL or osteoprotegerin (OPG).

What is known and what is new?

- It is known that patients with bone metastases have an increased RANKL gene expression and RANKL:OPG ratio. EVs are involved in organotrophic metastasis. *In vitro* analysis shows that NSCLC cells release exosomes which induce EGFR phosphorylation, leading to NSCLC-induced osteoclastogenesis and osteolytic bone invasion.
- We demonstrated that it is feasible to identify EVs using imaging flow cytometry and to determine RANKL and OPG plasma levels in archived long-term frozen plasma samples. Next to our key findings, our results indicate a trend toward improved overall survival in patients with lower EV counts.

What is the implication, and what should change now?

- As (RANKL+) EV counts significantly decrease during treatment, these could serve as a potential biomarker for *EGFR*+ NSCLC disease progression and response to therapy. Further research is needed to broaden these findings to NSCLC patients without an actionable driver mutation treated with e.g., chemotherapy or immunotherapy.

blood-based analysis.

Extracellular vesicles (EVs) are important in intracellular communication and the complex cascade of invasion-metastasis (3,4,11). These EVs contain lipids, nucleic acids, and proteins, as cargo, and are actively secreted by all cells within the human body. They can be classified based on their biogenesis pathways into apoptotic bodies exosomes, and microvesicles (4). EVs are involved in organotrophic metastasis, the phenomenon in which specific tumors exhibit a predilection for spreading and outgrowth at distinct distant metastatic sites and have been shown to influence the redirection of metastatic distribution (4,12). An *in vitro* study assessing the role of EVs in NSCLC bone metastasis revealed that NSCLC cells release exosomes containing EGFR ligand and amphiregulin (AREG), which induce EGFR phosphorylation. In turn, EGFR phosphorylation increases RANKL at both the mRNA and protein levels in pre-osteoclasts, leading to the upregulation of matrix metalloproteinase-9 (MMP-9) and tartrate-resistant acid phosphatase (TRAcP) expression, and possibly triggering osteoclastogenesis (13). These processes result in NSCLC-induced osteoclastogenesis and osteolytic bone invasion.

Rationale and knowledge gap

Our understanding of EVs *in vivo* remains limited. Small studies (n=27–35) including patients with lung cancer and healthy controls, and a rabbit lung cancer model showed that patients and rabbits with lung cancer exhibited higher levels of circulating EVs in comparison to healthy individuals (14,15). Research on EVs and their clinical translation is hindered by the absence of an established baseline value that could serve as a reference point for other studies. Multiple factors contribute to this, including variations in both the techniques used for EV isolation and quantification and a lack of clinical studies that can effectively translate the *in vitro* findings into clinical practice (16,17). Therefore, we initiated a clinical study to assess EVs in archived frozen plasma samples from patients with metastatic *EGFR*$^+$ NSCLC using a robust technique that has been demonstrated to detect single EVs in clinically, complex biofluids such as plasma without needing prior EV isolation, called imaging flow cytometry (IFC) (18).

Objective

The main objectives of this study were to investigate potential associations between (I) the levels of circulating EVs and the presence of bone metastases, and (II) the expression of RANKL on EVs in relation to bone metastases. The secondary objectives included evaluating the levels of RANKL and OPG proteins in the same plasma in relation to bone metastases and the association of total circulating EVs and RANKL$^+$ EVs, OPG and RANKL plasma levels to osimertinib treatment, presence of SREs and overall survival (OS). We present this article in accordance with the TREND reporting checklist (available at https://tlcr.amegroups.com/article/view/10.21037/tlcr-24-1007/rc).

Methods

This study involved the analysis of archived frozen plasma samples from patients with metastatic *EGFR*$^+$ NSCLC at the Erasmus Medical Center Cancer Institute.

Patient selection and data collection

This study used plasma samples of patients with *EGFR*$^+$ NSCLC enrolled in the prospective biomarker cohort study START-TKI (NCT05221372) (19). Patients were eligible for this study when harboring an activating *EGFR* mutation for which EGFR-tyrosine kinase inhibitor (EGFR-TKI) treatment was initiated. We included plasma samples of patients closest to the initiation of osimertinib treatment (≤6 weeks before initiation and at initiation) and during osimertinib treatment. At least one follow-up visit after initiation of osimertinib was required, otherwise patient samples were excluded.

The medical records of all patients, both inpatient and outpatient, were obtained. The following data were collected: demographics, date of first diagnosis and date of metastatic NSCLC, date of initiation and discontinuation of osimertinib, date of diagnosis, number and localization of bone metastases, presence of bone metastases at sample collection, presence of SREs (20) in patients with imaging confirmed bone metastases date and type of first SRE (if applicable), use of bone targeted agents, and date of death or last follow-up. Bone metastases diagnosed within 4 weeks of sample collection are considered to be present at the time of sample collection. Routine radiological evaluation was conducted every 2 to 3 months by chest and upper abdomen computer tomography (CT) scans with iodine contrast. The most recent follow-up date was May, 4, 2023.

The study was conducted in accordance with the Declaration of Helsinki (as revised in 2013). The study was approved by the Medical Ethics Review Committee

(MERC) of Erasmus Medical Center Cancer Institute (No. MEC 2016-643), and registered on ClinicalTrials.gov (No. NCT05221372). All patients provided informed consent.

Measurement of RANKL and OPG proteins in plasma

The protein levels of RANKL and OPG in plasma samples were measured by enzyme-linked immunosorbent assay (ELISA). For this, both human TRANCE/RANKL/TNFSF11 Duoset ELISA (R&D systems, Minneapolis, MN, USA; DY626) and human OPG/TNFRSF11B Duoset ELISA (R&D systems, DY805) were performed according to the manufacturer protocol. Thawed plasma samples were centrifuged for 5 minutes at 400 ×g before measurement and 100 µL plasma was taken from the top layer and pipetted in a 96-well ELISA plate coated with capture antibody diluted in phosphate-buffered saline (PBS). The OPG ELISA samples were first diluted 2 times in 1% bovine serum albumin in PBS. The RANKL ELISA samples were measured undiluted.

Measurement of EVs in plasma samples

IFC ImageStream®X Mk II instrument (Cytek Biosciences, Seattle, WA, USA) was performed according to the methodology of Woud *et al.* (18).

Monoclonal antibodies (mAbs) and isotype controls were vortexed and then 10 minutes centrifuged at 16,000 ×g to remove antibody aggregates. The antibodies were diluted in 0.22 µm filtered PBS (fPBS) to the working concentrations. In the supplemental data, Table S1 shows characteristics of the different antibodies.

Optimal TRANCE/RANKL mAb concentrations were determined by performing titration series in combination with CD9/CD63/CD81 tetraspanin expression in conditioned medium (CM) from human osteoblast (SV-HFO) cultures. The optimal concentration of RANKL mAb was determined as the concentration that gave the best distinction between sample [CM/platelet poor plasma (PPP)] and background (fPBS/PPP). The concentration of the tetraspanins mixture (CD9, CD63, and CD81) was adopted from Woud *et al.* (18). EVs were defined as tetraspanin positive events, and $RANKL^+$ EVs as both tetraspanin and $RANKL^+$ events.

Antibody staining was performed in 130 µL, consisting of 30 µL PPP, 12.5 µL of working solution of each of the tetraspanin mAbs, 12.5 µL of working solution containing RANKL mAb topped up with fPBS to 130 µL. After incubation overnight at 4 ℃ (dark), samples were set to a total volume of 380 µL using fPBS before IFC measurement. Controls that were taken along were fPBS only, fPBS with antibodies, fPBS with isotype controls, unstained PPP, PPP with isotype controls and detergent (10% v/v TritonX-100) treated PPP and fPBS. Detergent treatment was performed for 30 minutes at room temperature for all mAb stained PPP samples and four fPBS samples. The supplemental data includes figures detailing the identification of individual EVs.

Data acquisition and analysis were performed according to Woud *et al.* (18). In brief, the lasers used were 488 nm: 200 mW; 642 nm: 150 mW; side scatter (SSC): 1.25 mW. High gain mode was activated and data was acquired over 180 seconds for standardization between samples using the 60× objective with fluidics set to low speed/high sensitivity. The core size was set to 6 µm. RANKL fluorescence was detected in channel 2 (435–505 nm), allophycocyanin (APC) fluorescence in channel 5 (642–745 nm) and SSC signals in channel 6 (745–785 nm). Data analysis was performed using Amnis IDEAS software, version 6.2. To establish the analysis of single nanoparticles, all events with SSC intensities ≤900 arbitrary units (a.u.) were selected and events showing multiple fluorescent spots were excluded from analysis. With this gating strategy single spot fluorescent particles ≤400 nm were selected and analyzed (18).

Statistics

SPSS (v20; SPSS Inc., Chicago, IL, USA) was used for statistical analysis. Descriptive statistics of demographic and clinical variables were collected. All data underwent outlier detection, and in the presence of any identified outliers, they were subsequently removed from the dataset. Categorical variables were compared using Chi-squared tests or Fisher exact probability tests, and continuous variables were compared using the Mann-Whitney *U* test or Kruskall-Wallis test. The reverse Kaplan-Meier was used for calculating median follow-up time. The OS was calculated by Kaplan-Meier. Patients still alive were censored at the last day of follow-up.

Results

Patient characteristics

In total 50 plasma samples of 44 unique patients were available for analysis. Four patients were excluded as

Table 1 Patient characteristics

Characteristics	Data (n=40)
Female	22 [55]
Never smoker	10 [25]
Age at diagnosis metastatic NSCLC (years)	61.7 [43–78]
Mutation	
Common (exon 19 del, L858R, T790M)	38 [95]
Uncommon	2 [5]
Bone metastases present at sample collection	25 [63]
Bone metastases development after sample collection	6 [15]
Total number of patients with bone metastases during their disease span	31 [78]
SRE present at sample collection†	12/25 [48]
At least one SRE present†,‡	20/31 [65]
Treatment with bone targeted agents	2 [5]

Data are presented as n [%], mean [range], or n/total [%]. †, percentage was calculated in all patients with bone metastases; ‡, one patient had hypercalcemia, without bone metastases. Del, deletion; NSCLC, non-small cell lung cancer; SRE, skeletal related event.

their sample was obtained >6 weeks before initiation of osimertinib treatment, thus 40 patients were included in analysis. Plasma samples were stored at −80 ℃ for an average duration of 37.4 months.

All patients were not treatment-naive, rather treated with osimertinib in the second or later line. In 18 of 40 patients (45%) a plasma sample was available at initiation of osimertinib. In 22 out of 40 patients (55%) a plasma sample was only available during osimertinib treatment, which was obtained after a median duration of osimertinib treatment of 12.1 months (range, 0.7–43.5 months). Of the patients on treatment, 17/22 patients (77%) had an ongoing radiological response and 5/22 patients (23%) had disease progression at the time of sample collection. Patient characteristics are shown in *Table 1*. For clinical outcomes, the median follow-up from initiation of osimertinib treatment was 44.0 months [95% confidence interval (CI): 34.5–53.5].

Total and RANKL$^+$ positive EV concentrations at initiation and during osimertinib treatment

Identification of EVs from plasma was possible in 38 patients (95%). In two patients, the results were not replicable due to technical factors. Detection of EVs was based on their combined CD9/CD63/CD81 (tetraspanins) expression. The total concentration of EVs and the percentage of RANKL$^+$ EVs of the total EVs per patient were normally distributed, while the levels of RANKL$^+$ EVs and the intensity of RANKL expression were not (data not shown).

The total concentration of EVs was $4.5\times10^{12}\pm2.54\times10^{12}$/mL plasma [mean ± standard deviation (SD)]. The mean concentration of RANKL$^+$ EVs was $1.56\times10^{10}\pm1.02\times10^{10}$/mL plasma and RANKL$^+$ EVs were on average 0.5% of the total EV concentration per patient. Samples obtained at initiation of osimertinib showed significantly higher EV concentrations compared to samples obtained during treatment with osimertinib ($6.3\times10^{12}\pm2.1\times10^{12}$/mL plasma *vs.* $3.2\times10^{12}\pm1.9\times10^{12}$/mL plasma, $P\leq0.001$; *Figure 1A*). Similarly, RANKL$^+$ EV concentrations decreased significantly during treatment ($2.2\times10^{10}\pm9.3\times10^{9}$/mL plasma *vs.* $1.1\times10^{10}\pm8.0\times10^{9}$/mL plasma, P=0.001, *Figure 1B*). No difference was observed in RANKL intensity on RANKL$^+$ EVs at initiation or during treatment [median $7.0\times10^{6}\pm1.70\times10^{6}$ mean fluorescence intensity (MFI) *vs.* $8.5\times10^{6}\pm3.4\times10^{6}$ MFI, P=0.21; *Figure 1C*]. The percentage of RANKL$^+$ EVs of total EVs per patient was not significantly different at initiation or during treatment (0.4%±0.3% *vs.* 0.5%±0.5%, P=0.22; *Figure 1D*). *Figure 1E* presents a representative dot plot image of IFC data analysis of plasma EVs, comparing a patient at treatment initiation with a patient during treatment with osimertinib.

The median OS from start of osimertinib was 27.2 months (95% CI: 13.7–40.8) for patients with a high concentration of total EVs (defined as any value above the mean) and 48.9 months (95% CI: 22.8–74.9; P=0.56) for patients with a low concentration of EVs (defined as any value below the mean). The same trend was observed in patients with a high concentration of RANKL$^+$ EVs (defined as any value above the mean), as these patients had a median OS of 21.8 months (95% CI: 13.1–30.5). Whereas patients with a low concentration of RANKL$^+$ EVs (defined as any value below the mean), had a median OS of 42.3 months (95% CI: 31.6–53.0; P=0.13).

Total EV and RANKL$^+$ EV concentrations with or without bone metastases

The presence of bone metastases was not associated with the total concentration of EVs at the time of

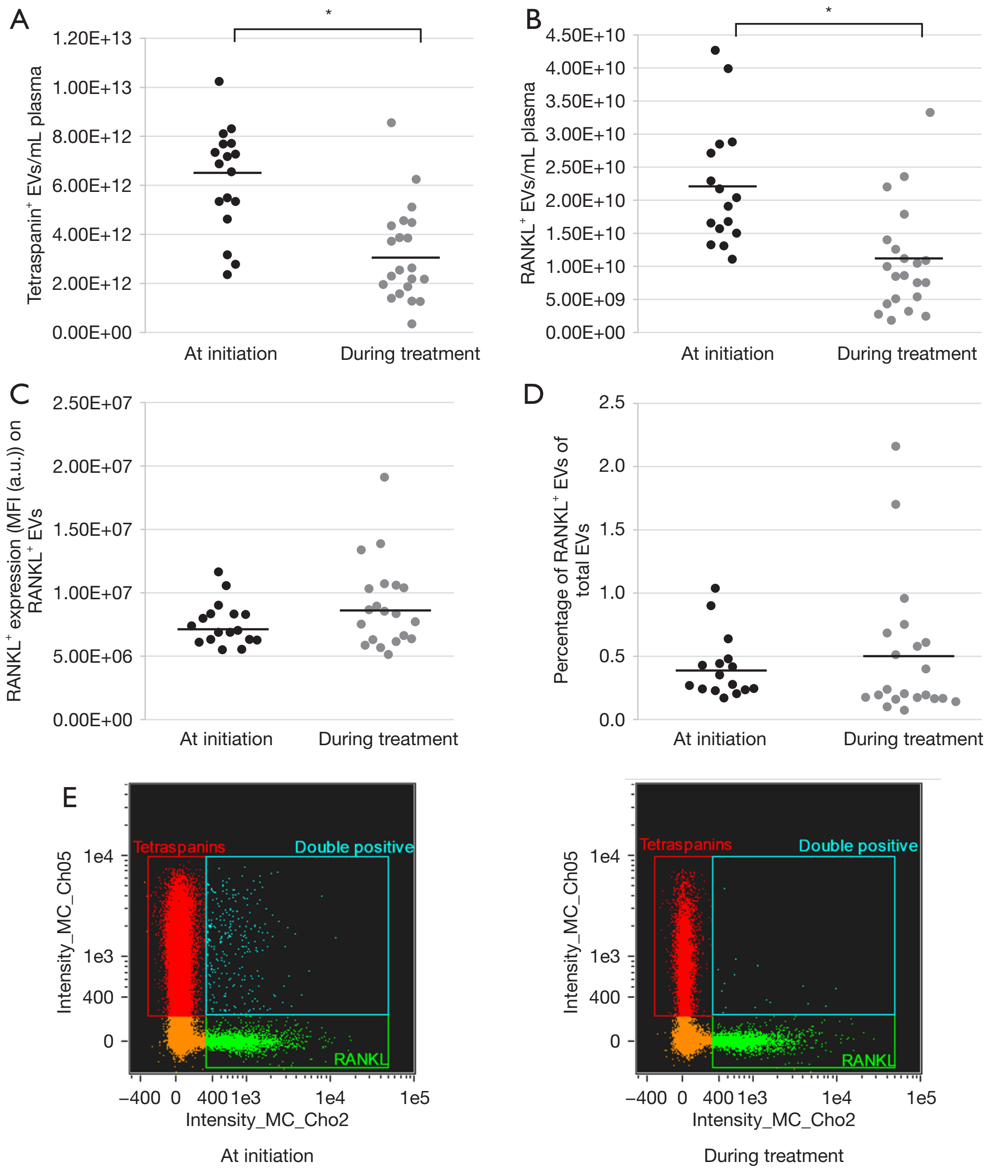

Figure 1 Distribution of EVs in plasma samples of patients at initiation of osimertinib therapy and during osimertinib therapy. (A) Total concentration of EVs. (B) Concentration of RANKL$^+$ EVs. (C) Intensity of RANKL expression on RANKL$^+$ EVs. (D) Percentage of RANKL$^+$ EVs of total EVs per patient. (E) Representative dot plot images of IFC data analysis of plasma EVs from a patient at initiation and a patient during treatment with osimertinib. Intensity_MC_Ch05 (Y-axis) shows the APC-conjugated tetraspanin signal and Intensity_MC_Ch02 (X-axis) shows the AF488 conjugated RANKL signal. Red boxes indicate the tetraspanin positive particles, blue boxes indicate particles that are tetraspanin positive and also RANKL positive (double positive). Green boxes show the RANKL positive particles that are not tetraspanin positive, in orange the negative particles are shown for both fluorochromes. All settings are based upon a series of controls shown in the Appendix 1. EVs are characterized as tetraspanin positive particles, RANKL$^+$ EVs as RANKL positive and tetraspanin positive particles (double positive). An asterisk (*) indicates a significant difference ($P<0.05$) between two groups, a horizontal line represents the mean in (A,B,D) or the median in (C). APC, allophycocyanin; a.u., arbitrary units; EVs, extracellular vesicles; MFI, median fluorescence intensity; OPG, osteoprotegerin; RANKL, receptor activator of nuclear factor κB ligand.

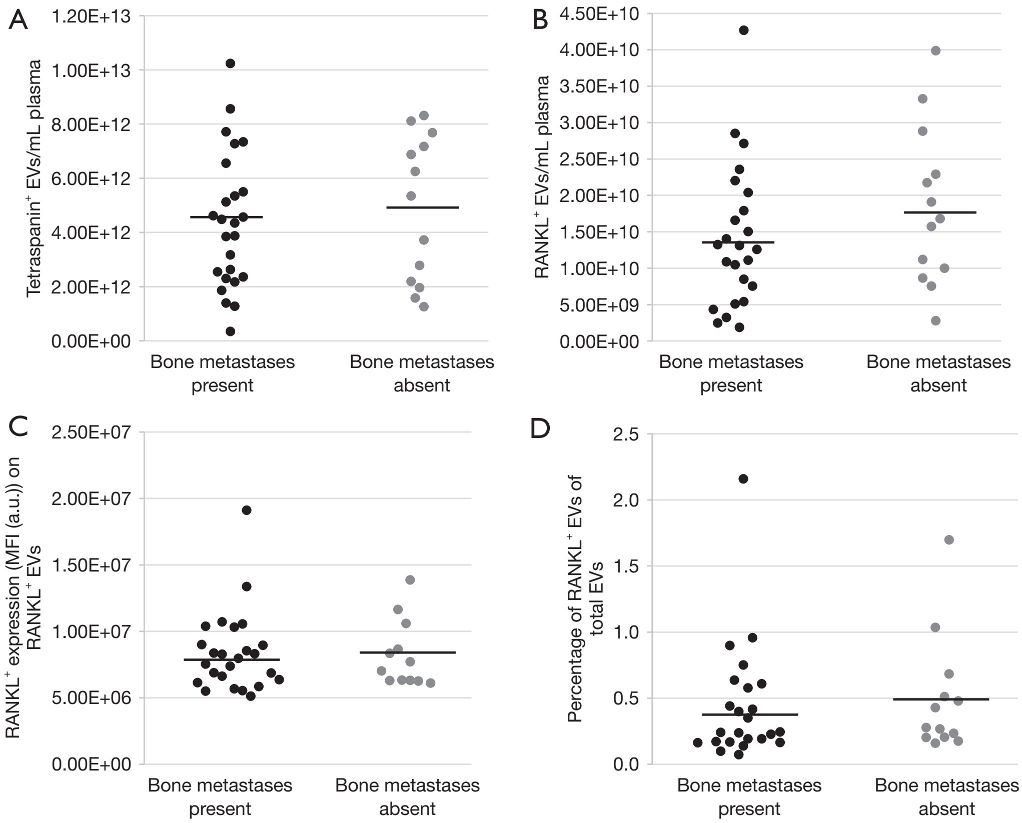

Figure 2 Distribution of EVs in plasma samples of patients with and without bone metastases at the time of sample collection. (A) Total concentration of EVs. (B) Concentration of RANKL$^+$ EVs. (C) Intensity of RANKL expression on RANKL$^+$ EVs. (D) Percentage of RANKL$^+$ EVs of total EVs per patient. A horizontal line represents the mean in (A,B,D) or the median in (C). A.u., arbitrary units; EVs, extracellular vesicles; MFI, median fluorescence intensity; OPG, osteoprotegerin; RANKL, receptor activator of nuclear factor κB ligand.

sample collection (4.4E+12±2.5E+12/mL plasma *vs.* 4.9E+12±2.7E+12/mL plasma, P=0.68; *Figure 2A*). Similarly, the concentration of RANKL$^+$ EVs was not significantly different between patients with or without bone metastases (1.4E+10±9.7E+9/mL plasma *vs.* 1.8E+10±1.1E+10/mL plasma, P=0.37; *Figure 2B*). There was no association between RANKL intensity on RANKL$^+$ EVs and the presence of bone metastases (median 8.0E+06±3.0E+06 MFI *vs.* 8.3E+06±2.5E+06 MFI, P=0.96; *Figure 2C*). The percentage of RANKL$^+$ EVs of the total EVs per patient was not significantly different for patients with and without bone metastases (0.4%±0.4% *vs.* 0.5%±0.4%, P=0.56; *Figure 2D*).

At the moment of sample collection, 12 patients of 25 bone metastasized patients (48%) had an SRE. The concentration of total EVs did not differ between the presence or absence of SREs (P=0.10; *Figure 3A*), however patients without an SRE had a significantly higher concentration of RANKL$^+$ EVs compared to patients with an SRE (mean 1.8E+10±1.1E+10/mL plasma *vs.* 1.1E+10±7.4E+09/mL plasma, P=0.02; *Figure 3B*). Whereas the RANKL intensity on RANKL$^+$ EVs and percentage of RANKL$^+$ EVs of the total EVs did not differ (P=0.10, P=0.54; *Figure 3C,3D*).

OPG and RANKL protein levels at initiation or during osimertinib therapy

OPG and RANKL plasma levels could be determined in all patient samples via ELISA. The OPG plasma levels were normally distributed, while the RANKL plasma levels were not (data not shown). For all patients, the median OPG plasma level was 1,869.0 ng/mL [interquartile range (IQR), 1,573.0–2,598.3 ng/mL] and the median RANKL plasma level was 117.8 ng/mL (IQR, 91.9–133.6 ng/mL).

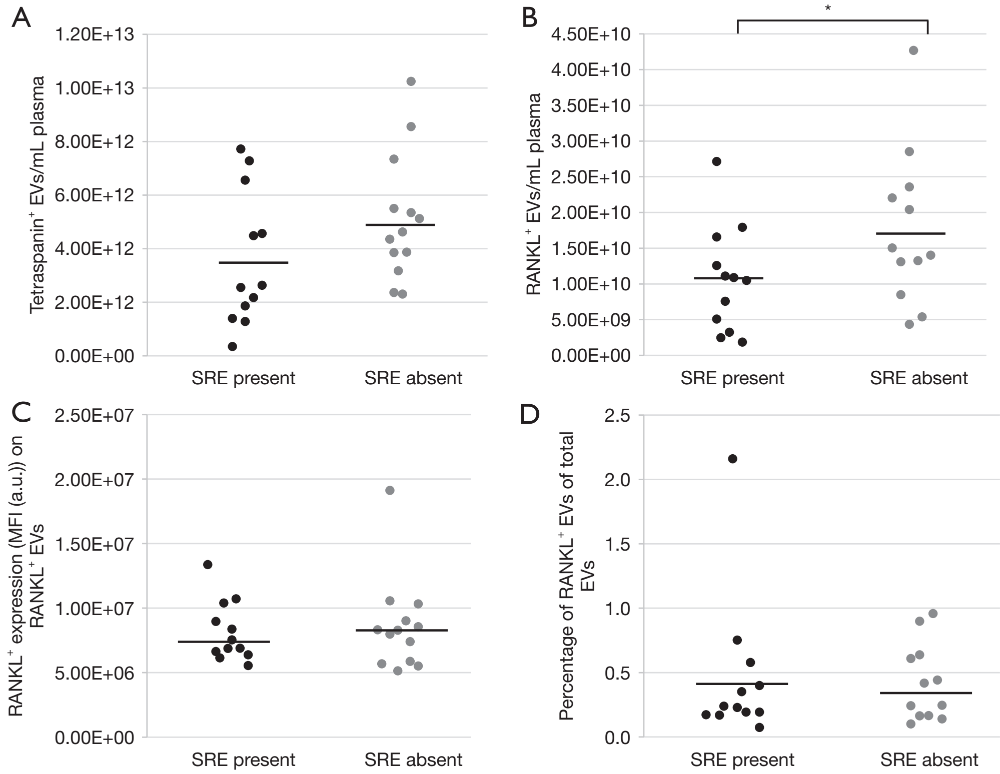

Figure 3 Distribution of EVs in plasma of patients with and without SREs at time of sample collection. (A) Total concentration of EVs. (B) Concentration of RANKL$^+$ EVs. (C) Intensity of RANKL expression on RANKL$^+$ EVs. (D) Percentage of RANKL$^+$ EVs of total EVs per patient. An asterisk (*) indicates a significant difference (P<0.05), a horizontal line represents the mean in (A,B,D) or the median in (C). A.u., arbitrary units; EVs, extracellular vesicles; MFI, median fluorescence intensity; OPG, osteoprotegerin; RANKL, receptor activator of nuclear factor κB ligand; SRE, skeletal related event.

The OPG and RANKL levels, or RANKL:OPG ratio were not significantly different between samples obtained at initiation or during osimertinib treatment (P=0.40, P=0.14, P=0.60; *Figure 4A-4C*).

OPG and RANKL protein levels with or without bone metastases

There was no statistically significant difference between OPG and RANKL levels in plasma and presence of bone metastases (P=0.053, P=0.23; *Figure 5A,5B*), however patients without bone metastases had a trend to lower OPG levels compared to patients with bone metastases. Patients without bone metastases had significantly increased RANKL:OPG ratios (P=0.009; *Figure 5C*). No significant differences were found between OPG and RANKL plasma levels, or RANKL:OPG ratio in patients with or without SREs (P=0.94, P=0.93, P=0.71).

Discussion

Key findings

This proof-of-concept study demonstrated the feasibility of identifying EVs using IFC and determining RANKL and OPG levels in plasma samples from patients with metastatic *EGFR*$^+$ NSCLC. We are unable to demonstrate a significant difference in the concentrations of circulating (RANKL$^+$) EVs or between plasma levels of OPG and RANKL in patients with and without bone metastases. However, the overall concentration of EVs and RANKL$^+$ EVs was significantly lower in samples collected during osimertinib treatment compared to those obtained at the initiation of osimertinib. This was not observed for OPG and RANKL plasma levels. In patients without SREs higher concentrations of RANKL$^+$ EVs were found, without any differences in total concentrations of EVs and height of RANKL expression on RANKL$^+$ EVs. Our results

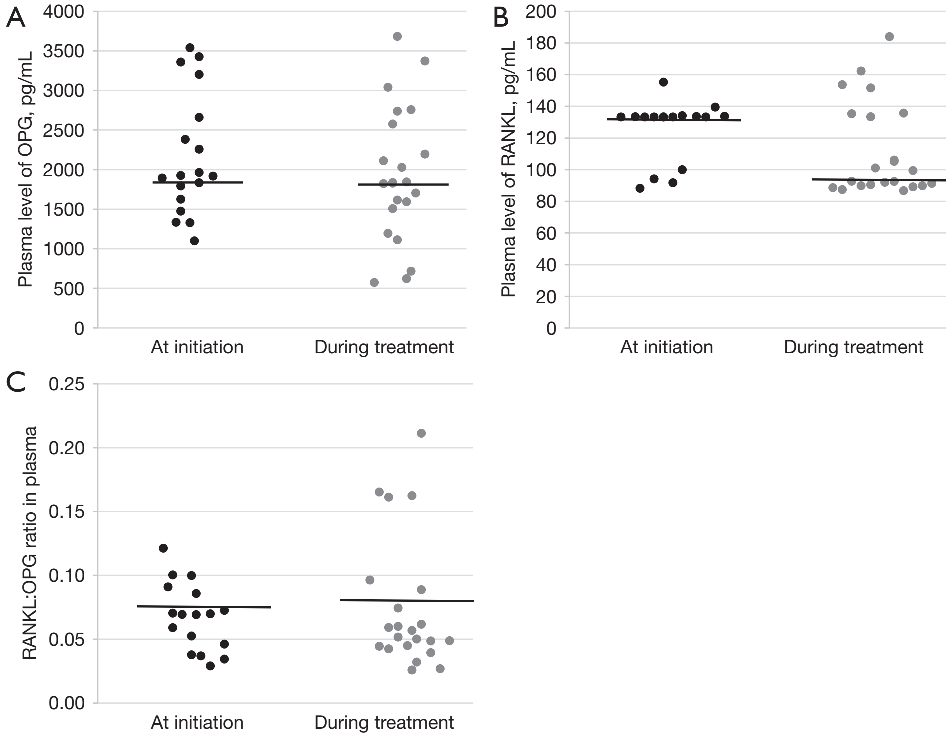

Figure 4 Distribution of OPG and RANKL protein levels, and RANKL:OPG ratio in plasma of patients at initiation of osimertinib therapy and during osimertinib therapy. (A) Plasma level of OPG (pg/mL). (B) Plasma level of RANKL (pg/mL). (C) RANKL:OPG ratio in plasma. A horizontal line represents the median in (A,B), or the mean in (C). RANKL and OPG protein levels were measured via ELISA. ELISA, enzyme-linked immunosorbent assay; OPG, osteoprotegerin; RANKL, receptor activator of nuclear factor κB ligand.

indicate a trend toward improved OS in patients with lower total concentrations of EVs and lower concentrations of RANKL$^+$ EVs.

Strengths and limitations

This study establishes a reproducible method for identifying and quantifying EVs in the plasma of patients with NSCLC using archived long-term frozen samples. This approach avoids imposing additional diagnostic burdens on a vulnerable patient population. Additionally, the RANKL and OPG levels obtained are consistent with findings from studies using fresh plasma (21), and the EV counts in patient samples are higher than those reported in healthy individuals. This suggests that utilizing frozen plasma does not compromise the reliability of the results.

However, several limitations should be acknowledged. First, the relatively small sample size and the disproportionate ratio of patients with and without bone metastases (1.7:1) may introduce bias, although the high incidence of bone metastases in this population highlights the importance of ongoing research in this area. Furthermore, our study included only non-treatment-naive patients, and samples were collected during osimertinib treatment, which may have affected EV concentrations and impacted the results.

Comparison with similar researches

In the last decade, there has been increasing attention on EV research due to their potential as biomarkers, therapeutic targets, or drug delivery systems (12,22,23). However, the analysis of EVs presents significant challenges and these challenges may have influenced our results. EV associated challenges stem from various factors, including their small size, the diversity of protein markers depending on the cell source, the low abundance of pathological EVs, and the absence of unique antigens that represent specific EV classes (18). In addition, the identification of EVs in blood plasma is impeded by the molecular complexity of plasma, which contains diverse particles that can interfere

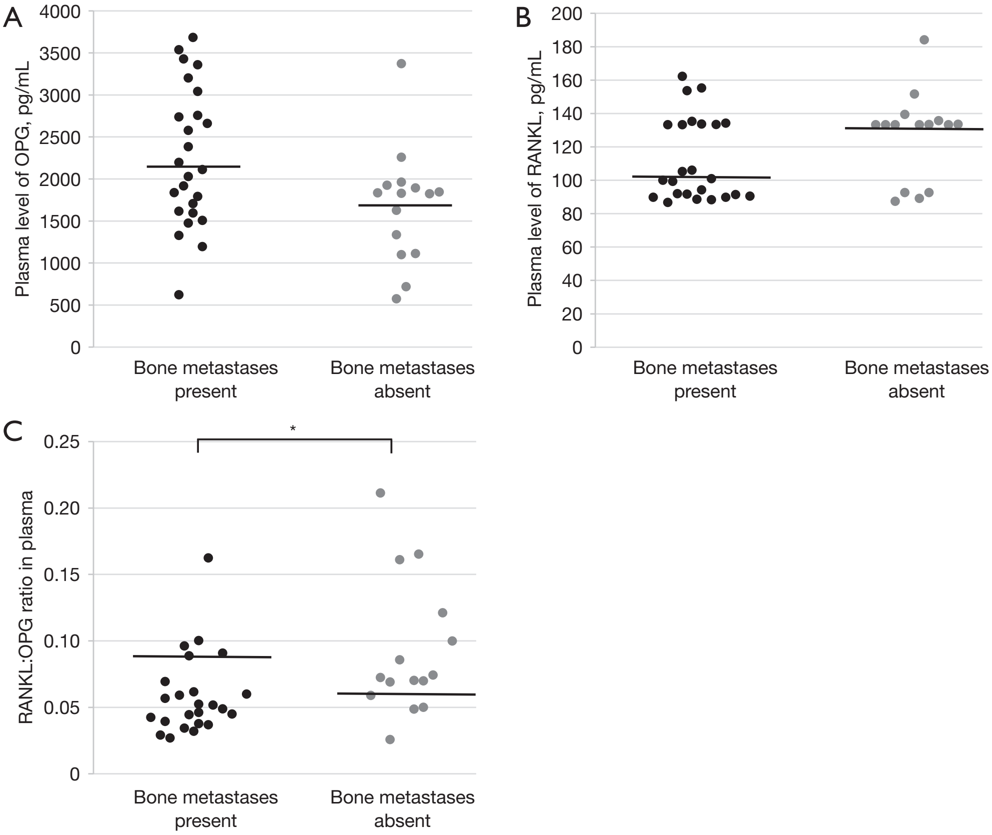

Figure 5 Distribution of OPG and RANKL protein levels, and RANKL:OPG ratio in plasma of patients with and without bone metastases at time of sample collection. (A) Plasma level of OPG (pg/mL). (B) Plasma level of RANKL (pg/mL). (C) RANKL:OPG ratio in plasma. An asterisk (*) indicates a significant difference between the two groups (P<0.05). A horizontal line represents the median in (A,B), or the mean in (C). OPG, osteoprotegerin; RANKL, receptor activator of nuclear factor κB ligand.

with EV analysis (18). Currently, there is no established gold standard method for detecting and distinguishing individual EVs. To the best of our knowledge, our study is the first to measure EV concentrations in patients with NSCLC using IFC. Consequently, we could not directly compare the EV concentrations to other (NSCLC) studies in humans. A previous study in which the individual EVs of five healthy humans were quantified using IFC, reported a mean EV concentration of ~2E+08 objects per mL, which is lower compared with our results (18). Due to the absence of plasma samples from healthy controls in our study population and because we used the high gain setting during acquisition of the samples, a direct comparison with our results is not possible. The lower EV concentrations in healthy individuals are consistent with earlier research in which higher EVs concentrations were observed in patients with NSCLC compared to healthy controls (15,24).

The lower EV and RANKL$^+$ EV concentration in samples collected during osimertinib treatment, validate those seen in an *in vitro* study involving an *EGFR* mutant NSCLC cell line, in which EV concentration drops following treatment of the NSCLC cells with osimertinib (25). The decrease in EV concentration mirrors the post-resection scenario in glioblastoma, where increased concentrations of EVs in patients revert to levels comparable to those of healthy controls after glioblastoma resection (26). However, the lower concentrations of EVs during treatment contrast with the observation in patients undergoing chemotherapy, where chemotherapy can induce vesicle release and alter their cargo (27,28).

The presence of bone metastases was not associated with plasma levels of OPG and RANKL. These findings are in contrast with another study, as the predictive role of serum levels of OPG and RANKL in detecting bone metastases have been established in a study involving 80 patients with breast cancer (with and without bone metastases) (29). They showed that an increased RANKL:OPG ratio of >0.14 had an appropriate sensitivity and specificity (73% and 72%) in detection of bone metastases (29). Serum values of RANKL and OPG are affected not only by malignancy or bone metastases but also by various factors, including infectious diseases, age, cardiovascular comorbidity, or diabetes (21,30-34). Furthermore, aside from its role in bone turnover, OPG also plays a role in regulating cancer cell invasion. Elevated serum OPG levels have been observed in patients with metastatic NSCLC, resulting in upregulation of miRNA-20a, which promotes NSCLC cell invasion (35). Besides that, OPG has the capacity to bind to the tumor necrosis factor-related apoptosis inducing ligand (TRAIL), thus preventing the interaction between TRAIL and its death receptors and blocking TRAIL-induced apoptosis (31). All of these factors could potentially influence our results, however due to the small sample sizes, we were unable to correct for these variables.

Explanations of findings

We found that the concentration of EV per milliliter plasma was substantial in all patients, but we could not demonstrate a significant difference in total concentrations of EVs between patients with and without bone metastases. This might be explained by the disproportionate ratio between patients with and without bone metastases, the fact that none of the patients was treatment-naive, or by the reduction in concentration of EVs during treatment. In patients without SREs higher concentrations of RANKL$^+$ EVs were found, without any differences in total concentrations of EVs and height of RANKL expression on RANKL$^+$ EVs. A plausible explanation for this finding is that in patients with an SRE, RANKL$^+$ EVs are already present in the bone microenvironment. In contrast, in patients without SREs, these RANKL$^+$ EVs are still found in the plasma. The overall concentration of EVs and RANKL$^+$ EVs was significantly lower in samples collected during osimertinib treatment compared to samples obtained at initiation of osimertinib. Interestingly, there was no difference between the percentage of RANKL$^+$ EVs relative to the total EVs between initiation and during treatment. Consequently, the decrease in RANKL$^+$ EVs is likely attributable to the overall decline in EV concentration. The decrease in EV concentration is plausibly associated with a response to treatment, given that 77% of the patients had an ongoing response.

Our hypothesis was that there was an association between the EV concentrations and bone metastases, given EVs' role in organotropism but we could not demonstrate this, potential reasons were discussed above (36). Additionally, it is possible that integrins, which are transmembrane receptors that promote cell adhesion and migration of the cargo of EVs, or the cargo of the vesicle (including miRNA and proteins), play a more significant role in preparing the metastatic niche for bone metastasis development rather than the number of EVs or their membrane expression of RANKL (36). It would be interesting to further explore the relation between EV cargo (e.g., membrane expression of RANK and EGFR, or intracellular expression of EGFR) and presence of bone metastases in new experiments. Other studies showed a reduced OS for patients with a high concentration of EVs (24,37). We observed only a trend towards decreased OS in patients with a high concentration of EVs compared to those with a lower concentration. However, likely owing to the limited sample sizes, inclusion of non-treatment-naive patients, and obtaining samples during osimertinib treatment, this did not reach statistical significance. If the concentration of EVs and RANKL$^+$ EVs is indeed associated with response on treatment and/or survival, this would represent a prognostic parameter. In case of total EV concentration, this might be easily implemented in routine laboratory tests.

Implications and actions needed

The aforementioned limitations highlight the need for further investigation in larger, more balanced cohorts to validate the findings regarding the lower concentrations of EVs and RANKL$^+$ EVs in relation to treatment response

Conclusions

No association was found between the presence of bone metastases and the total concentration of EVs, RANKL$^+$ EVs or plasma levels of RANKL and OPG. However, the total concentration of EVs and RANKL$^+$ EVs in plasma declines during treatment with osimertinib, while in patients without SREs there is an increase in RANKL$^+$ EVs concentration. Our study shows the importance of EV signatures in NSCLC patient plasma as future prognostic parameters.

Acknowledgments

This study is part of A.J.W.M.B.'s dissertation (May 2024)

and has not been published elsewhere.

Footnote

Reporting Checklist: The authors have completed the TREND reporting checklist. Available at https://tlcr.amegroups.com/article/view/10.21037/tlcr-24-1007/rc

Data Sharing Statement: Available at https://tlcr.amegroups.com/article/view/10.21037/tlcr-24-1007/dss

Peer Review File: Available at https://tlcr.amegroups.com/article/view/10.21037/tlcr-24-1007/prf

Funding: None.

Conflicts of Interest: All authors have completed the ICMJE uniform disclosure form (available at https://tlcr.amegroups.com/article/view/10.21037/tlcr-24-1007/coif). A.J.W.M.B. has received a travel grant from the ELCC, and she have participated in an advisory board for Jansen (payment was paid to A.J.W.M.B.). C.M.J.S. has received research funding from AstraZeneca, stichting NVALT studies, ICON Clinical Research/Arcus biosciences, VitroScan Leiden (payment was paid to institution), consulting fees from BMS (payment was paid to institution), honoraria from iDoctor and Benecke (payment was paid to institution) and C.M.J.S. received uncompensated relationships from Eli Lily (payment was paid to C.M.J.S.). A.M.C.D. has received grants or contracts from Amgen, Dutch Cancer Society and Hanart, consulting fees from Amgen, Bayer, Boehringer Ingelheim, Sanofy, Roche, Johnson&Johnson, Astra Zeneca, Pfizer and Mirati, honor from Janssen, Pfizer, Astra Zeneca, Lilly and Amgen. All payments were paid to the institution. A.M.C.D. takes part in a data safety monitoring board or advisory board from Takeda, Roche and Lilly (all payments were paid to the institution). A.M.C.D. is chair from EORTC LCG, unpaid. L.E.L.H. has received research fundings from Roche Genentech, AstraZeneca, Boehringer Ingelheim, Takeda, Merck, Pfizer, Novartis, Gilead (all payments were paid to institution), honor for speaker educationals/webinars from AstraZeneca, Bayer, Lilly, MSD, high5oncology, Takeda, Janssen, GSK, Sanofi, Pfizer (all payments were paid to institution) and from Medtalks, Benecke, VJOncology, Medimix (payments were paid to LEL Hendriks). She took part in advisory boards from Abbvie, Amgen, Anhearth, AstraZeneca, Bayer, BMS, Boehringer Ingelheim, Daiichi, GSK, Janssen, Lilly, Merck, MSD, Novartis, Pfizer, Pierre Fabre, Roche, Sanofi, Summit Therapeutics, Takeda (all payments were paid to institution). L.E.L.H. is the member of guideline committees of Dutch guidelines on NSCLC, brain metastases and leptomeningeal metastases (payment to L.E.L.H.), ESMO guidelines on metastatic NSCLC, non-metastatic NSCLC and SCLC (non-financial), other (non-financial): secretary NVALT studies foundation, subchair EORTC metastatic NSCLC systemic therapy, vice-chair scientific committee Dutch Thoracic Group. L.E.L.H. is local PI of clinical trials from AstraZeneca, GSK, Novartis, Merck, Roche, Takeda, Blueprint, Mirati, Abbvie, Gilead, MSD, Amgen, Boehringer Ingelheim and Pfizer (all payments were paid to institution). The other authors have no conflicts of interest to declare.

Ethical Statement: The authors are accountable for all aspects of the work in ensuring that questions related to the accuracy or integrity of any part of the work are appropriately investigated and resolved. The study was conducted in accordance with the Declaration of Helsinki (as revised in 2013). The study was approved by the institutional Medical Ethics Review Committee (MERC) of Erasmus Medical Center Cancer Institute (No. MEC 2016-643), and registered on ClinicalTrials.gov (No. NCT05221372). All patients provided informed consent.

References

1. Longkanker Nederland. Cijfers over longkanker. 2022. Available online: https://www.longkankernederland.nl/longkanker/statistieken
2. Park HK, Han J, Kwon GY, et al. Patterns of Extrathoracic Metastasis in Lung Cancer Patients. Curr Oncol 2022;29:8794-801.
3. Obenauf AC, Massagué J. Surviving at a Distance: Organ-Specific Metastasis. Trends Cancer 2015;1:76-91.
4. Urabe F, Patil K, Ramm GA, et al. Extracellular vesicles in

the development of organ-specific metastasis. J Extracell Vesicles 2021;10:e12125.
5. Kuijpers CCHJ, Hendriks LEL, Derks JL, et al. Association of molecular status and metastatic organs at diagnosis in patients with stage IV non-squamous non-small cell lung cancer. Lung Cancer 2018;121:76-81.
6. Brouns AJWM, Hendriks LEL, Robbesom-van den Berge IJ, et al. Association of RANKL and EGFR gene expression with bone metastases in patients with metastatic non-small cell lung cancer. Front Oncol 2023;13:1145001.
7. Kang Y. Dissecting Tumor-Stromal Interactions in Breast Cancer Bone Metastasis. Endocrinol Metab (Seoul) 2016;31:206-12.
8. Schneider MR, Sibilia M, Erben RG. The EGFR network in bone biology and pathology. Trends Endocrinol Metab 2009;20:517-24.
9. Yi T, Lee HL, Cha JH, et al. Epidermal growth factor receptor regulates osteoclast differentiation and survival through cross-talking with RANK signaling. J Cell Physiol 2008;217:409-22.
10. Hofman P. The challenges of evaluating predictive biomarkers using small biopsy tissue samples and liquid biopsies from non-small cell lung cancer patients. J Thorac Dis 2019;11:S57-64.
11. Nogués L, Benito-Martin A, Hergueta-Redondo M, et al. The influence of tumour-derived extracellular vesicles on local and distal metastatic dissemination. Mol Aspects Med 2018;60:15-26.
12. Cheng L, Hill AF. Therapeutically harnessing extracellular vesicles. Nat Rev Drug Discov 2022;21:379-99.
13. Taverna S, Pucci M, Giallombardo M, et al. Amphiregulin contained in NSCLC-exosomes induces osteoclast differentiation through the activation of EGFR pathway. Sci Rep 2017;7:3170.
14. Rabinowits G, Gerçel-Taylor C, Day JM, et al. Exosomal microRNA: a diagnostic marker for lung cancer. Clin Lung Cancer 2009;10:42-6.
15. Choi BH, Quan YH, Rho J, et al. Levels of Extracellular Vesicles in Pulmonary and Peripheral Blood Correlate with Stages of Lung Cancer Patients. World J Surg 2020;44:3522-9.
16. Johnsen KB, Gudbergsson JM, Andresen TL, et al. What is the blood concentration of extracellular vesicles? Implications for the use of extracellular vesicles as blood-borne biomarkers of cancer. Biochim Biophys Acta Rev Cancer 2019;1871:109-16.
17. Cappello F, Fais S. Extracellular vesicles in cancer pros and cons: The importance of the evidence-based medicine. Semin Cancer Biol 2022;86:4-12.
18. Woud WW, van der Pol E, Mul E, et al. An imaging flow cytometry-based methodology for the analysis of single extracellular vesicles in unprocessed human plasma. Commun Biol 2022;5:633.
19. Steendam CMJ, Veerman GDM, Pruis MA, et al. Plasma Predictive Features in Treating EGFR-Mutated Non-Small Cell Lung Cancer. Cancers (Basel) 2020;12:3179.
20. Kuchuk M, Addison CL, Clemons M, et al. Incidence and consequences of bone metastases in lung cancer patients. J Bone Oncol 2013;2:22-9.
21. Martinez LM, Vallone VB, Labovsky V, et al. Changes in the peripheral blood and bone marrow from untreated advanced breast cancer patients that are associated with the establishment of bone metastases. Clin Exp Metastasis 2014;31:213-32.
22. Goberdhan DCI. Large tumour-derived extracellular vesicles as prognostic indicators of metastatic cancer patient survival. Br J Cancer 2023;128:471-3.
23. Carreca AP, Tinnirello R, Miceli V, et al. Extracellular Vesicles in Lung Cancer: Implementation in Diagnosis and Therapeutic Perspectives. Cancers (Basel) 2024;16:1967.
24. Vetsika EK, Sharma P, Samaras I, et al. Small Extracellular Vesicles in Pre-Therapy Plasma Predict Clinical Outcome in Non-Small-Cell Lung Cancer Patients. Cancers (Basel) 2021;13:2041.
25. Stridfeldt F, Cavallaro S, Hååg P, et al. Analyses of single extracellular vesicles from non-small lung cancer cells to reveal effects of epidermal growth factor receptor inhibitor treatments. Talanta 2023;259:124553.
26. Osti D, Del Bene M, Rappa G, et al. Clinical Significance of Extracellular Vesicles in Plasma from Glioblastoma Patients. Clin Cancer Res 2019;25:266-76.
27. Ab Razak NS, Ab Mutalib NS, Mohtar MA, et al. Impact of Chemotherapy on Extracellular Vesicles: Understanding the Chemo-EVs. Front Oncol 2019;9:1113.
28. Lee YJ, Chae S, Choi D. Monitoring of single extracellular vesicle heterogeneity in cancer progression and therapy. Front Oncol 2023;13:1256585.
29. Elfar GA, Ebrahim MA, Elsherbiny NM, et al. Validity of Osteoprotegerin and Receptor Activator of NF-κB Ligand for the Detection of Bone Metastasis in Breast Cancer. Oncol Res 2017;25:641-50.
30. Kudlacek S, Schneider B, Woloszczuk W, et al. Serum levels of osteoprotegerin increase with age in a healthy adult population. Bone 2003;32:681-6.
31. Wang Y, Liu Y, Huang Z, et al. The roles of osteoprotegerin in cancer, far beyond a bone player. Cell

Death Discov 2022;8:252.
32. Abid S, Lee M, Rodich B, et al. Evaluation of an association between RANKL and OPG with bone disease in people with cystic fibrosis. J Cyst Fibros 2023;22:140-5.
33. Granchi D, Garaventa A, Amato I, et al. Plasma levels of receptor activator of nuclear factor-kappaB ligand and osteoprotegerin in patients with neuroblastoma. Int J Cancer 2006;119:146-51.
34. Natsag J, Kendall MA, Sellmeyer DE, et al. Vitamin D, osteoprotegerin/receptor activator of nuclear factor-kappaB ligand (OPG/RANKL) and inflammation with alendronate treatment in HIV-infected patients with reduced bone mineral density. HIV Med 2016;17:196-205.
35. Wan K, Tu Z, Liu Z, et al. Upregulated osteoprotegerin expression promotes lung cancer cell invasion by increasing miR-20a expression. Exp Ther Med 2021;22:846.
36. Hurwitz SN, Meckes DG Jr. Extracellular Vesicle Integrins Distinguish Unique Cancers. Proteomes 2019;7:14.
37. Nanou A, Miller MC, Zeune LL, et al. Tumour-derived extracellular vesicles in blood of metastatic cancer patients associate with overall survival. Br J Cancer 2020;122:801-11.

Cite this article as: Brouns AJWM, Robbesom-van den Berge IJ, Ernst SM, Steendam CMJ, Woud WW, Wu L, Dingemans AMC, Hendriks LEL, van Driel M. Connecting the dots: (RANKL$^+$) extracellular vesicle count in blood plasma in relation to bone metastases, skeletal related events and osimertinib treatment in patients with EGFR mutated non-small cell lung cancer. Transl Lung Cancer Res 2025;14(3):761-774. doi: 10.21037/tlcr-24-1007